

Substituted *N*-picolylenediamines of the type (ArNHCH₂CH₂)-{(2-C₅H₄N)CH₂}NR [R = Me, 4-CH₂=CH(C₆H₄)CH₂, (2-C₅H₄N)CH₂] and their transition metal(II) halide complexes

Christopher J. Davies,^a John Fawcett,^a Richard Shutt^b and Gregory A. Solan^{*a}

^a Department of Chemistry, University of Leicester, University Road, Leicester, UK LE1 7RH.

E-mail: gas8@leicester.ac.uk

^b ExxonMobil Chemical Europe, Hermeslaan 2, B-1831 Machelen, Belgium

Received 25th April 2005, Accepted 20th June 2005

First published as an Advance Article on the web 4th July 2005

Alkylation of (ArNHCH₂CH₂){(2-C₅H₄N)CH₂}NH with RX [RX = MeI, 4-CH₂=CH(C₆H₄)CH₂Cl] and (2-C₅H₅N)CH₂Cl in the presence of base has allowed access to the sterically demanding multidentate nitrogen donor ligands, {(2,4,6-Me₃C₆H₂)NHCH₂CH₂}{(2-C₅H₄N)CH₂}NMe (**L1**), {(2,6-Me₂C₆H₃)NHCH₂CH₂}{(2-C₅H₄N)CH₂}NCH₂(C₆H₄)-4-CH=CH₂ (**L2**) and (ArNHCH₂CH₂){(2-C₅H₄N)CH₂}₂N (Ar = 2,4-Me₂C₆H₃, **L3a**, 2,6-Me₂C₆H₃, **L3b**) in moderate yield. **L3** can also be prepared in higher yield by the reaction of (NH₂CH₂CH₂)-{(2-C₅H₄N)CH₂}₂N with the corresponding aryl bromide in the presence of base and a palladium(0) catalyst. Treatment of **L1** or **L2** with MCl₂ [MCl₂ = CoCl₂·6H₂O or FeCl₂(THF)_{1.5}] in THF affords the high spin complexes [(**L1**)MCl₂] (M = Co **1a**, Fe **1b**) and [(**L2**)MCl₂] (M = Co **2a**, Fe **2b**) in good yield, respectively; the molecular structure of **1a** reveals a five-coordinate metal centre with **L1** bound in a facial fashion. The six-coordinate complexes, [(**L3a**)MCl₂] (M = Co **3a**, Fe **3b**, Mn **3c**) are accessible on treatment of tripodal **L3a** with MCl₂. In contrast, the reaction with the more sterically encumbered **L3b** leads to the *pseudo*-five-coordinate species [(**L3b**)MCl₂] (M = Co **4a**, Fe **4b**) and, in the case of manganese, dimeric [(**L3b**)MnCl(μ-Cl)]₂ (**4c**); in **4a** and **4b** the aryl-substituted amine arm forms a partial interaction with the metal centre while in **4c** the arm is pendant. The single crystal X-ray structures of **1a**, **3b**·MeCN, **3c**·MeCN, **4b**·MeCN and **4c** are described as are the solution state properties of **3b** and **4b**.

1 Introduction

The emergence in recent years of tridentate nitrogen donor ligand frames that can act as compatible supports for both early (Ti, Zr, V, Cr)¹⁻⁴ and late (Fe, Co)^{5,6} transition metal-based olefin polymerisation catalysts has fuelled a considerable research activity directed towards the design of alternative ligand frameworks.⁷ In many cases the *N,N,N*-chelates are symmetrically disposed [e.g., bis(imino)pyridines,³⁻⁶ bis(amido)pyridines,² bis(amido)amines¹] with the exterior nitrogen donors possessing aryl substituents which impart, through both steric and electronic variation, considerable control on the resultant catalyst performance.

Recently we have reported the synthesis of both iron and cobalt halide complexes containing the highly flexible (both *mer*- and *fac*-configurations accessible) mono-aryl-substituted *N*-picolylenediamine frame (Fig. 1) which, on activation with MAO, are active catalysts for the oligomerisation of ethylene.⁸ These type of ligands are of added interest due to the scope for further functionalisation such as at the central nitrogen atom. This functionalisation could, for example, include the introduction of simple alkyl groups (to modify the electronic properties) through to the incorporation of a polymerisable side arm⁹ to allow immobilisation on an organic support.

Alternatively, an additional donor group could be introduced to augment the denticity of the ligand.

This manuscript is concerned, in the first instance, with the synthesis of methylated **L1**, pendant arm-containing **L2** and tripodal **L3** (Fig. 1). Secondly, the synthesis and detailed characterisation of paramagnetic metal chloride complexes supported by **L1-L3** is described including X-ray structural characterisation of cobalt, iron and manganese complexes.

2 Results and discussion

2.1 Derivatised *N*-Picolylenediamine ligands

The reaction of RX [RX = MeI, 4-CH₂=CH(C₆H₄)CH₂Cl] and (2-C₅H₅N)CH₂Cl with the corresponding aryl-substituted *N*-picolylenediamine, (ArNHCH₂CH₂){(2-C₅H₄N)CH₂}NH,⁸ in the presence of excess K₂CO₃ gives {(2,4,6-Me₃C₆H₂)NHCH₂CH₂}{(2-C₅H₄N)CH₂}NMe (**L1**), {(2,6-Me₂C₆H₃)NHCH₂CH₂}{(2-C₅H₄N)CH₂}NCH₂(C₆H₄)-4-CH=CH₂ (**L2**) and (ArNHCH₂CH₂){(2-C₅H₄N)CH₂}₂N (Ar = 2,4-Me₂C₆H₃, **L3a**, 2,6-Me₂C₆H₃, **L3b**) in yields between 38–63% (Scheme 1). Also identified as by-products in the formation of **L1-L3** are the corresponding ammonium salts

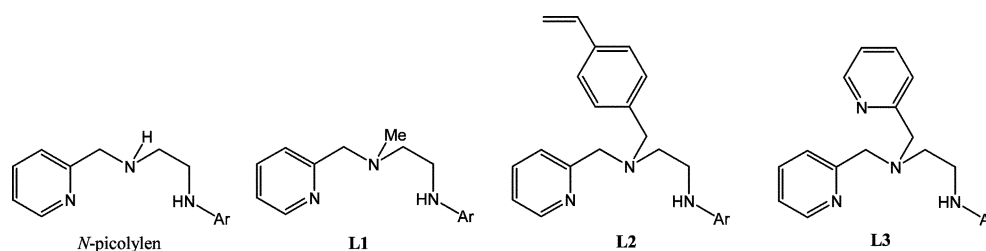
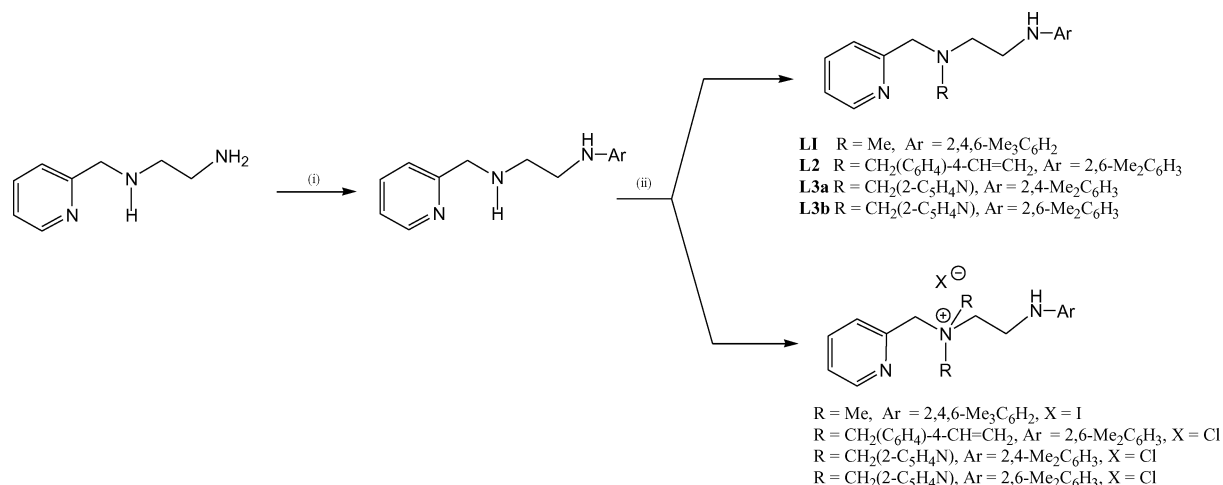
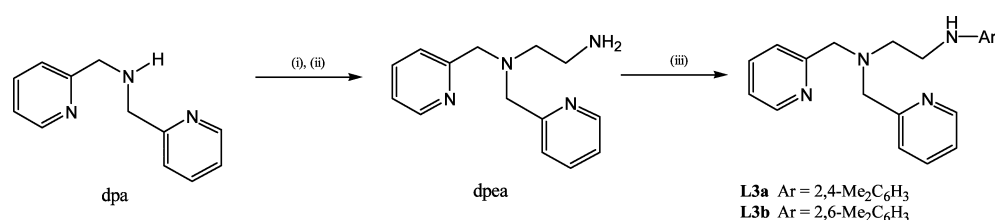


Fig. 1 *N*-picolylen and its derivatives (**L1**, **L2** and **L3**) reported in this study.



Scheme 1 Reagents and conditions: (i) Ar–Br, NaOBU^t, Pd₂(dba)₃ (0.2 mol%), *rac*-BINAP, toluene, heat;⁸ (ii) RX, xs. K₂CO₃, MeCN, –10 to 20 °C (**L1**), 80 °C (**L2**) or 55 °C (**L3**).



Scheme 2 Reagents and conditions: (i) *N*-tosylaziridine, CH₃CN, heat; (ii) conc. H₂SO₄, heat; (iii) Ar–Br, NaOBU^t, Pd₂(dba)₃ (0.2 mol%), *rac*-BINAP, toluene, heat.

which can be readily separated following chromatography on alumina.

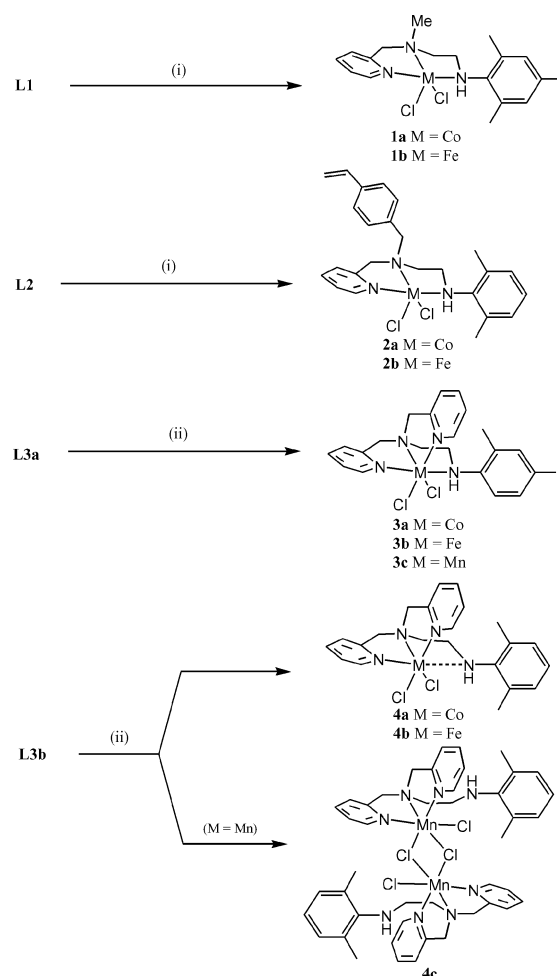
Alternatively, **L3** can be prepared in two steps from *N,N*-bis(2-picolyl)amine (dpa).¹⁰ Firstly, dpa can be converted to *N,N*-dipicolylethylenediamine (dpea) using previously reported procedures¹¹ or by reacting dpa with *N*-tosylaziridine¹² followed by tosyl deprotection under acidic conditions (Scheme 2). Secondly, treatment of dpea with one equivalent of the corresponding aryl bromide in the presence of a catalytic amount of Pd₂(dba)₃ gave **L3a** and **L3b** as the sole products in good yield.¹³ All the new ligands have been characterised by IR, ¹H and ¹³C NMR spectroscopy and ES mass spectrometry (see Experimental section).

2.2 Complexes of L1–L3

Treatment of MCl₂ [MCl₂ = CoCl₂·6H₂O, FeCl₂(THF)_{1.5}] with one equivalent of **L1** or **L2** in tetrahydrofuran at room temperature affords [(**L1**)MCl₂] (M = Co **1a**, Fe **1b**) and [(**L2**)MCl₂] (M = Co **2a**, Fe **2b**) in good yield (Scheme 3). All the complexes have been characterised by mass spectrometry, IR spectroscopy and magnetic measurements (Table 1). In addition, **1a** has been the subject of a single crystal X-ray diffraction study.

Purple crystals of **1a** suitable for the X-ray diffraction study were grown by slow cooling of a hot acetonitrile solution of **1a**. The molecular structure of **1a** is depicted in Fig. 2; selected bond distances and bond angles are listed in Table 2.

The structure of **1a** consists of a single cobalt atom surrounded by a facially bound tridentate nitrogen donor ligand and two monodentate chloride ligands. The coordination geometry can be best described as distorted trigonal bipyramidal with the equatorial plane being defined by N(1)_{pyridyl}, N(3)_{arylamine}, Cl(2) [N(1)–Co(1)–N(3) 104.82(16)°, N(1)–Co(1)–Cl(2) 110.09(13)°, N(3)–Co(1)–Cl(2) 139.68(12)°] and the axial sites by N(2) and Cl(1) [N(2)–Co(1)–Cl(1) 166.88(12)°]. The *N*-aryl group is oriented such that the *ortho*-methyl groups [C(16) and C(18)] are positioned above and below the plane defined by N(2)–Co(1)–N(3)–C(9) [max. deviation from plane N(3) 0.0232 Å]



Scheme 3 Reagents and conditions: (i) MCl₂ [MCl₂ = CoCl₂·6H₂O or FeCl₂(THF)_{1.5}], THF, room temperature; (ii) MCl₂, *n*-BuOH, 90 °C.

Table 1 Spectroscopic and analytical data for the new complexes **1–4**

Compound	$\mu_{\text{eff}}/\text{BM}^a$	$\nu(\text{N-H})/\text{cm}^{-1b}$	FAB mass spectrum	Microanalysis (%) ^c		
				C	H	N
1a	4.09	3278	789 [2M – Cl] ⁺ , 412 [M] ⁺ , 377 [M – Cl] ⁺	52.63 (52.30)	6.16 (6.05)	10.09 (10.17)
1b	5.11	3281	785 [2M – Cl] ⁺ , 410 [M] ⁺ , 374 [M – Cl] ⁺	52.91 (52.69)	6.23 (6.10)	10.11 (10.24)
2a	4.16	3263	967 [2M – Cl] ⁺ , 465 [M – Cl] ⁺	60.01 (59.89)	5.95 (5.79)	8.47 (8.38)
2b	5.09	3274	960 [2M – Cl] ⁺ , 462 [M – Cl] ⁺	^d	^d	^d
3a	4.26	3290	917 [2M – Cl] ⁺ , 440 [M/2 – Cl] ⁺	55.71 (55.46)	5.62 (5.46)	11.69 (11.76)
3b	5.22	3279	910 [2M – Cl] ⁺ , 472 [M] ⁺ , 437 [M – Cl] ⁺	55.80 (55.84)	5.59 (5.54)	11.67 (11.84)
3c	5.76	3311, 3261	909 [2M – Cl] ⁺ , 436 [M – Cl] ⁺	55.73 (55.95)	5.67 (5.55)	11.67 (11.86)
4a	3.97	3241	917 [2M – Cl] ⁺ , 440 [M – Cl] ⁺ , 405 [M – 2Cl] ⁺	55.29 (55.46)	5.41 (5.46)	11.51 (11.76)
4b	5.31	3238	909 [2M – Cl] ⁺ , 472 [M] ⁺ , 437 [M – Cl] ⁺	55.67 (55.84)	5.46 (5.54)	12.00 (11.84)
4c	8.04	3312, 3261	909 [M – Cl] ⁺ , 436 [M/2 – Cl] ⁺	55.81 (55.95)	5.37 (5.55)	11.88 (11.86)

^a Recorded on an Evans Balance at room temperature ^b Recorded on a Perkin-Elmer Spectrum One FT-IR spectrometer on solid samples ^c Calculated values are shown in parentheses ^d The microanalytical data for **2b** were repeatedly incorrect.

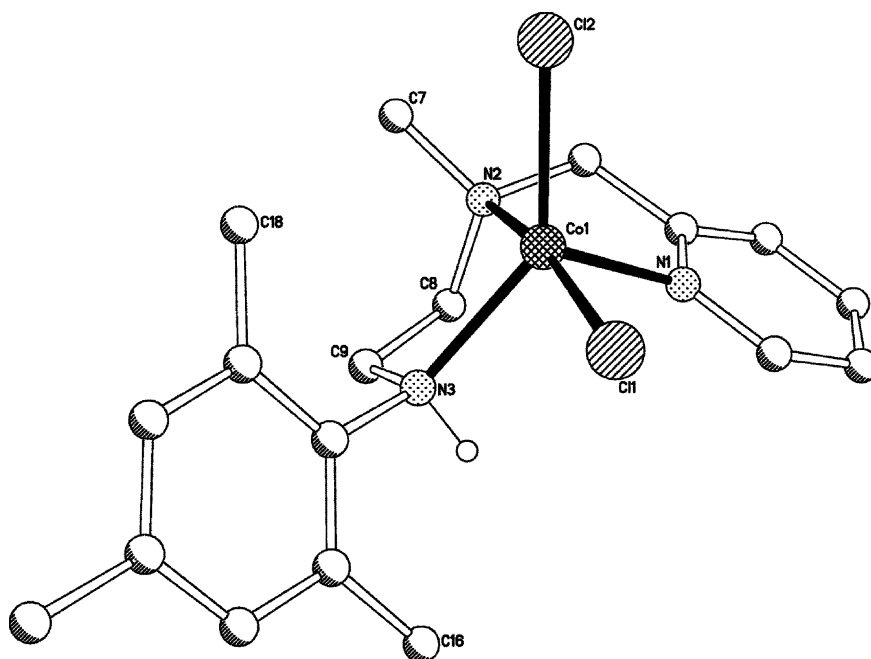
Table 2 Selected bond distances (Å) and angles (°) for **1a**

Co(1)–N(1)	2.093(4)	Co(1)–Cl(1)	2.3107(15)
Co(1)–N(2)	2.254(4)	Co(1)–Cl(2)	2.3159(15)
Co(1)–N(3)	2.170(4)		
N(1)–Co(1)–N(2)	76.42(17)	N(3)–Co(1)–Cl(1)	90.95(12)
N(1)–Co(1)–N(3)	104.82(16)	N(1)–Co(1)–Cl(2)	110.09(13)
N(2)–Co(1)–N(3)	79.45(16)	N(2)–Co(1)–Cl(2)	89.59(12)
N(1)–Co(1)–Cl(1)	97.73(13)	N(3)–Co(1)–Cl(2)	139.68(12)
N(2)–Co(1)–Cl(1)	166.88(12)	Cl(1)–Co(1)–Cl(2)	103.48(6)

with the C(18)_{o-Me} group pointing in a similar direction to Cl(2). The three Co–N distances are inequivalent with the Co–N(pyridyl) distance being the shortest [Co(1)–N(1) 2.093(4) Å] and the distance involving the central tertiary amine the longest [Co(1)–N(2) 2.254(4) Å]. In comparison with the non-methylated analogue, $\{[(2,4,6\text{-Me}_3\text{C}_6\text{H}_2)\text{NHCH}_2\text{CH}_2]\{(2\text{-C}_5\text{H}_4\text{N})\text{CH}_2\}\text{NH}\}\text{CoCl}_2\}$,⁸ the presence of the central methyl-substituted tertiary nitrogen donor in **1a** has the effect of elongating both the Co–N bond [by 0.065(4) Å] and the Co–Cl(axial) bond [by 0.028(1) Å]; the Co–N(arylamine) and the Co–Cl(equatorial) bonds are,

however, contracted by 0.044(4) and 0.045(1) Å, respectively. In contrast, the Co–N(pyridyl) distance is essentially the same in both structures as is the Cl–Co–Cl angle at [103.48(6)° (**1a**) vs. 103.11(3)°]. Due to the centric nature of the space group, both R/R and S/S forms are present for the two chiral centres at N(2) and N(3) in the crystal of **1a**, a relative configuration that is also observed in $\{[(\text{ArNHCH}_2\text{CH}_2)\{(2\text{-C}_5\text{H}_4\text{N})\text{CH}_2\}\text{NH}\}\text{CoCl}_2\}$ (Ar = 2,6-Me₂C₆H₃, 2,4,6-Me₃C₆H₂).⁸

The FAB mass spectrum for **1a**, along with those for **1b**, **2a** and **2b**, give molecular ion peaks and/or fragmentation peaks corresponding to the loss of chloride ions from the molecular ion and, in addition, minor peaks that can be attributed to dimeric species. In their IR spectra the $\nu(\text{N-H})$ absorption bands are seen at *ca.* 3274 cm⁻¹ and shifted (by *ca.* 75 cm⁻¹) to a lower wavenumber in comparison with that observed in the corresponding free ligands. The $\nu(\text{C}=\text{C})$ band for **2a** and **2b** is seen at *ca.* 1626 cm⁻¹ and shows little variation in wavenumber when compared to that found in free **L2**. The magnetic susceptibility measurements for the cobalt complexes, **1a** and **2a**, reveal magnetic moments of *ca.* 4.13 BM (Evans Balance at ambient temperature) which are consistent with high spin configurations possessing three unpaired electrons (*S* = 3/2). On the other hand, **1b** and **2b** exhibit moments of *ca.* 5.1

**Fig. 2** Molecular structure of **1a**. All hydrogen atoms except for H1 have been omitted for clarity.

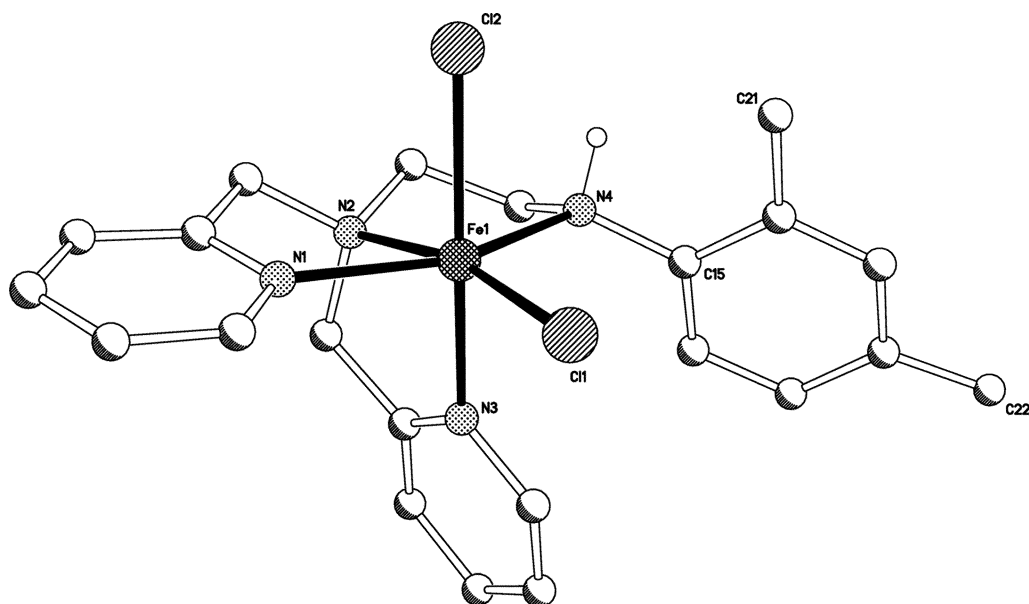


Fig. 3 Molecular structure of **3b**. All hydrogen atoms except for H4 have been omitted for clarity.

BM, consistent with high spin configurations possessing four unpaired electrons ($S = 2$).

Interaction of anhydrous MCl_2 with one equivalent of **L3a** at 90 °C in *n*-butanol gives $[(L3a)MCl_2]$ ($M = Co$ **3a**, Fe **3b**, Mn **3c**) while reaction of MCl_2 with **L3b** affords $[(L3b)MCl_2]$ ($M = Co$ **4a**, Fe **4b**) and $[(L3b)MnCl(\mu-Cl)]_2$ (**4c**) in high yield (Scheme 3). All the compounds have been characterised by FAB mass spectrometry, magnetic susceptibility measurements, IR spectroscopy and elemental analysis (Table 1). Furthermore, crystals of **3b**, **3c**, **4b** and **4c** have been the subject of single crystal X-ray diffraction studies.

Yellow crystals of **3b** and clear crystals of **3c** suitable for the X-ray studies were grown by either slow cooling of a hot acetonitrile solution containing the complex or by layering an acetonitrile solution with hexane, respectively. Despite the apparent immiscibility of acetonitrile and hexane, we have found that crystals of **3c** could not be grown from acetonitrile

alone. The structures of **3b** and **3c** are essentially identical, both containing two unique molecules (A and B) differing mainly in the inclination of the aryl groups; only one of the unique molecules in **3b** will be discussed in any detail. The molecular structure of **3b** is shown in Fig. 3 while selected bond distances and bond angles for both **3b** and **3c** (molecules A and B for each) are listed in Table 3. The structure comprises a single iron atom surrounded by a *N,N,N,N*-tripod and two monodentate chloride ligands so as to complete a distorted octahedral environment. One of the two pyridyl donors in the *N,N,N,N*-tripod is located *trans* to Cl(2) [$N(3)-Fe(1)-Cl(2)$ 165.55(18)°] while the other is *trans* to the 2,4-Me₂Ph-substituted amine [$N(1)-Fe(1)-N(4)$ 150.9(2)°] leaving the tertiary amine atom and Cl(1) mutually *trans* [$N(2)-Fe(1)-Cl(1)$ 167.69(19)°]. Of the four M–N bond distances the two involving the pyridyl nitrogen atoms are the shortest [Fe(1)–N(1) 2.191(7), Fe(1)–N(3) 2.169(7) Å], followed by the one involving the tertiary

Table 3 Selected bond distances (Å) and angles (°) for **3b**-MeCN and **3c**-MeCN

	3b -MeCN (M = Fe)		3c -MeCN (M = Mn)	
	Molecule A	Molecule B	Molecule A	Molecule B
M(1)–N(1)	2.191(7)	2.175(7)	2.272(7)	2.252(7)
M(1)–N(2)	2.249(6)	2.231(7)	2.344(7)	2.340(7)
M(1)–N(3)	2.169(7)	2.192(7)	2.279(7)	2.285(7)
M(1)–N(4)	2.303(6)	2.319(6)	2.400(6)	2.383(7)
M(1)–Cl(1)	2.337(2)	2.299(2)	2.400(2)	2.369(2)
M(1)–Cl(2)	2.468(2)	2.536(2)	2.472(2)	2.529(2)
N(1)–M(1)–N(2)	74.2(2)	73.8(2)	71.7(2)	71.7(2)
N(1)–M(1)–N(3)	95.0(2)	91.6(2)	93.7(2)	90.1(3)
N(1)–M(1)–N(4)	150.9(2)	152.2(2)	146.7(2)	148.0(2)
N(2)–M(1)–N(3)	76.7(2)	77.1(2)	74.4(2)	74.3(2)
N(2)–M(1)–N(4)	77.2(2)	78.6(2)	75.3(2)	76.4(2)
N(3)–M(1)–N(4)	83.6(2)	85.7(2)	81.3(2)	83.8(2)
N(1)–M(1)–Cl(1)	100.28(18)	99.17(19)	101.38(18)	99.40(18)
N(2)–M(1)–Cl(1)	167.69(19)	169.09(18)	163.86(17)	164.94(19)
N(3)–M(1)–Cl(1)	93.02(18)	95.13(19)	91.95(18)	93.98(18)
N(4)–M(1)–Cl(1)	108.82(16)	108.68(17)	111.61(16)	112.32(17)
N(1)–M(1)–Cl(2)	90.55(18)	94.81(18)	92.01(17)	95.54(19)
N(2)–M(1)–Cl(2)	91.99(17)	90.23(17)	93.15(17)	90.95(18)
N(3)–M(1)–Cl(2)	165.55(18)	163.57(19)	163.80(18)	161.72(19)
N(4)–M(1)–Cl(2)	85.08(16)	81.55(17)	85.62(17)	82.23(17)
Cl(1)–M(1)–Cl(2)	99.15(8)	98.75(8)	101.77(8)	102.18(9)

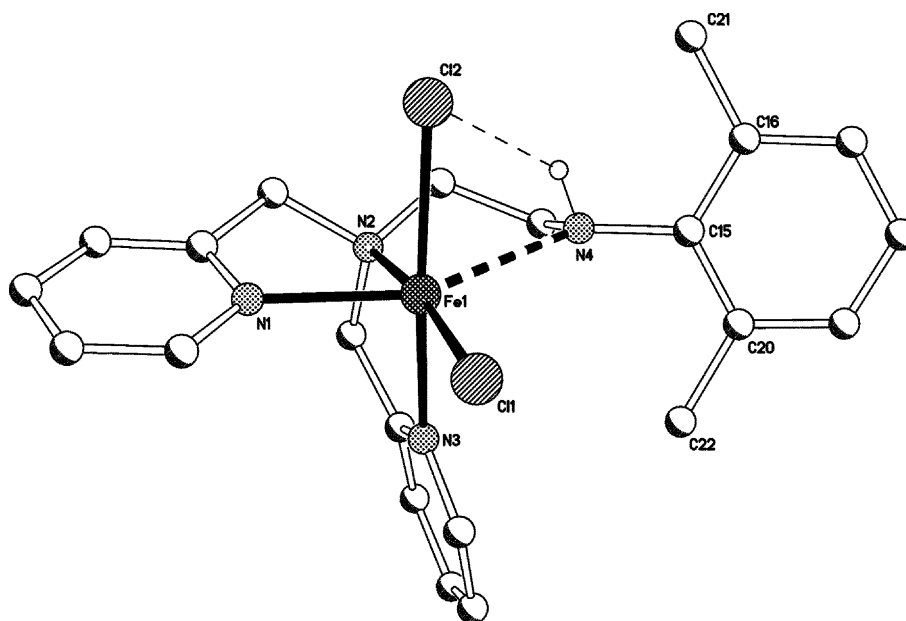


Fig. 4 Molecular structure of **4b**. All hydrogen atoms except for H4 have been omitted for clarity.

amine [Fe(1)–N(2) 2.249(6) Å] and the most elongated distance involving the aryl-substituted amine [Fe(1)–N(4) 2.303(6) Å]. This *cis*-arrangement of the pyridyl donors in **3b** is in contrast to the *trans*-configuration observed for [(dpea)Fe(NCS)₂]^{11a} but resembles the configuration seen in [(dpea)Mn(μ-O)₂](ClO₄)₃.¹⁴ The M–Cl bond distances are inequivalent, presumably due to the differing *trans* effects imposed on each chloride ligand (*tert*-amine vs. pyridyl) with M(1)–Cl(2) bond distance being the longest [2.468(2) Å].

The FAB mass spectra of **3a–c** gave molecular ion peaks and/or fragmentation peaks corresponding to the loss of chloride ions from their [M]⁺ peaks. As with **1** and **2**, **3a–c** all show minor peaks corresponding to the loss of a chloride from a dimeric species. The magnetic susceptibility measurements (Evans Balance at ambient temperature) for **3a–c** indicate high spin configurations are present in each case giving magnetic moments consistent with three (**3a**), four (**3b**) and five (**3c**) unpaired electrons. In the IR spectra of **3a–c**, characteristic pyridyl ring deformation bands at *ca.* 1600 cm⁻¹ are observed along with absorption bands for the bound N(Ar)–H groups (*ca.* 3280 cm⁻¹).

Golden crystals of **4b** suitable for the X-ray diffraction study were grown by slow cooling of a hot acetonitrile solution containing the complex. The molecular structure of **4b** is shown in Fig. 4; selected bond distances and bond angles are listed in Table 4. The structure resembles **3b** with a single iron centre surrounded by a *N,N,N,N*-tripod and two monodentate chloride ligands. However, effective coordination of the 2,6-Me₂Ph-substituted amine (N4) donor is impeded

as a response to the steric interactions between a pyridyl group and one *ortho*-Me group (C22) with the result that N4 forms only a weak interaction with Fe(1) [Fe(1)⋯N(4) 2.5580(16) *cf.* Fe(1)–N(4) 2.303(6) Å (**3b**)]. This weak interaction is likely to be further supplemented by a hydrogen-bonding interaction between H(4) and Cl(2) [*ca.* 2.358 Å]. As a consequence the geometry of the metal centre can be described as somewhere between octahedral and square pyramidal. It is noteworthy that a similar elongation has been observed in the related mesityl-substituted ferrous complex [((2,4,6-Me₃C₆H₂)NHCH₂CH₂)₂{(2-C₅H₄N)CH₂}N}FeCl₂]¹⁵ in which the corresponding Fe⋯N distance is 2.597(5) Å. The elongation in **4b** seems to have a minimal effect on the MCl₂ unit with the Cl(1)–Fe(1)–Cl(2) angle [97.20(2) *vs.* 99.15(8)° (**3b**)] and the M–Cl bond distances [Fe(1)–Cl(1), 2.3203(6) *vs.* 2.337(2)° (**3b**); Fe(1)–Cl(2), 2.4627(6) *vs.* 2.468(2)° (**3b**)] similar to that in **3b**. Conversely, the coordinated M–N distances in **4b** vary considerably with Fe–N(*tert*-amine) being compressed by *ca.* 0.078 Å, while Fe–N(pyridyl) distances are lengthened and most significantly for the pyridyl donor *trans* to the loosely bound aryl-substituted amine (*ca.* 0.073 Å). As with **3b**, the Fe–N bond distances are all >2.0 Å, characteristic of high spin ferrous complexes.¹⁶

Clear crystals of **4c** were grown by layering of an acetonitrile solution with hexane. The molecular structure of **4c** is shown in Fig. 5; selected bond distances and bond angles are listed in Table 5. Unlike **4b**, the structure of **4c** consists of a dimeric unit generated through a crystallographically imposed

Table 4 Selected bond distances (Å) and angles (°) for **4b**·MeCN

Fe(1)–N(1)	2.1712(16)	Fe(1)⋯N(4)	2.5580(16)
Fe(1)–N(2)	2.2636(16)	Fe(1)–Cl(1)	2.3203(6)
Fe(1)–N(3)	2.1883(16)	Fe(1)–Cl(2)	2.4627(6)
N(1)–Fe(1)–N(2)	74.91(6)	N(3)–Fe(1)–Cl(1)	93.68(5)
N(1)–Fe(1)–N(3)	91.02(6)	N(4)⋯Fe(1)–Cl(1)	108.81(5)
N(1)–Fe(1)⋯N(4)	147.70(5)	N(1)–Fe(1)–Cl(2)	92.72(4)
N(2)–Fe(1)–N(3)	77.81(6)	N(2)–Fe(1)–Cl(2)	91.53(4)
N(2)–Fe(1)⋯N(4)	74.41(5)	N(3)–Fe(1)–Cl(2)	167.38(5)
N(3)–Fe(1)⋯N(4)	92.32(5)	N(4)⋯Fe(1)–Cl(2)	78.10(3)
N(1)–Fe(1)–Cl(1)	103.12(5)	Cl(1)–Fe(1)–Cl(2)	97.20(2)
N(2)–Fe(1)–Cl(1)	171.15(4)		

Table 5 Selected bond distances (Å) and angles (°) for **4c**

Mn(1)–N(1)	2.3907(16)	Mn(1)–Cl(2)	2.5706(7)
Mn(1)–N(2)	2.2876(17)	Mn(1)–Cl(2A)	2.5321(7)
Mn(1)–N(3)	2.2226(16)	Mn(1)⋯Mn(1A)	3.795(1)
Mn(1)–Cl(1)	2.4279(6)		
N(1)–Mn(1)–N(3)	72.67(6)	N(3)–Mn(1)–Cl(2)	87.43(4)
N(1)–Mn(1)–N(2)	70.30(6)	N(1)–Mn(1)–Cl(2A)	91.92(4)
N(2)–Mn(1)–N(3)	97.18(6)	N(2)–Mn(1)–Cl(2A)	88.31(4)
N(1)–Mn(1)–Cl(1)	157.94(4)	N(3)–Mn(1)–Cl(2A)	160.58(4)
N(2)–Mn(1)–Cl(1)	93.76(4)	Cl(1)–Mn(1)–Cl(2)	96.75(2)
N(3)–Mn(1)–Cl(1)	95.18(5)	Cl(1)–Mn(1)–Cl(2A)	103.06(2)
N(1)–Mn(1)–Cl(2)	100.91(4)	Cl(2)–Mn(1)–Cl(2A)	83.91(2)
N(2)–Mn(1)–Cl(2)	168.11(4)	Mn(1)–Cl(2)–Mn(1A)	96.09(2)

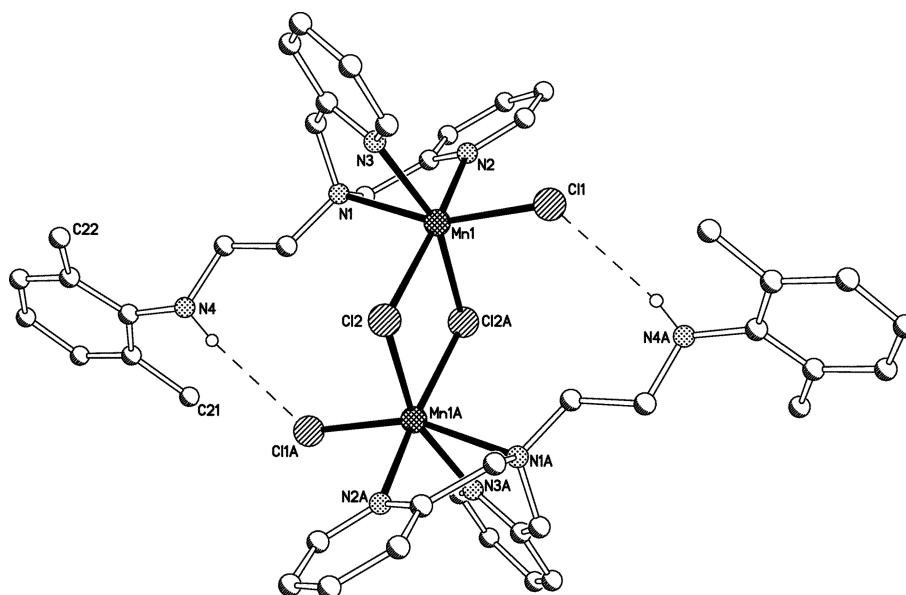


Fig. 5 Molecular structure of **4c**; the atoms labelled with an additional A are generated by symmetry ($2 - x, -y, 1 - z$). All hydrogen atoms except for H4 have been omitted for clarity.

inversion centre. The two manganese centres are bridged by a pair of chloride ligands and bound terminally by both a chloride and **L3b** to give a distorted octahedral geometry at each metal centre. **L3b** acts as a tridentate ligand and adopts a facial configuration [N(2)–Mn(1)–N(3) 97.18(6)°] with the 2,6-Me₂Ph-substituted amine non-coordinated. The structure of **4c** resembles that of [(Etdpa)MnCl(μ-Cl)]₂ (Etdpa = ethyl-substituted dipicolylamine)¹⁷ in which the central tertiary amines are *trans* to a terminal chloride and the pyridyl groups are *trans* to the bridging chlorides. As expected the Mn–N(amine) bond distance in **4c** [Mn(1)–N(1) 2.3907(16) Å] is longer than the Mn–N(pyridyl) bond distances [Mn(1)–N(2) 2.2876(17), Mn(1)–N(3) 2.2226(16) Å]. The two Mn–μ-Cl bond distances are slightly different [Mn(1)–Cl(2) 2.5706(7), Mn(1)–Cl(2A) 2.5321(7) Å] and longer than the terminal Mn–Cl bond distances [Mn(1)–Cl(1) 2.4279(6) Å]. The ClMn(μ-Cl)₂MnCl motif has been found in a number of crystallographically characterised complexes with the transannular Mn...Mn separation of 3.795(1) Å falling in the mid-range.¹⁸ While no notable intermolecular interactions are apparent, there is evidence that weak N(Ar)–H...Cl interactions occur intramolecularly between the pendant amine hydrogen atom and a terminal chloride ligand (*ca.* 2.654 Å).

The IR spectra for **4a–c** reflect the ligand coordination modes within the complexes by exhibiting characteristic pyridyl ring deformation bands at *ca.* 1600 cm⁻¹ and N–H stretching frequencies in the range 3312–3238 cm⁻¹. In **4a** and **4b** the single broad N–H absorption bands are seen at the lower end of the range and shifted by *ca.* 100 cm⁻¹ with regard to free **L3b**. In **4c**, however, two bands are seen at 3312 and 3261 cm⁻¹ in an approximate intensity ratio of 3 : 1, respectively. It is likely that the higher wavenumber band corresponds to the pendant N(Ar)–H groups in dimeric **4c** while the lower wavenumber band to a monomeric isomer analogous in structure to **4a** and **4b**. Interestingly, in **3c** two peaks are also observed in the NH region (3311 and 3261 cm⁻¹); in this case a preference for the lower wavenumber absorption band is observed (*ca.* 4 : 1). The room temperature magnetic susceptibility measurements of **4a–c** all indicate high spin behaviour with three [Co(II), *S* = 3/2] and four [Fe(II), *S* = 2] unpaired electrons present in **4a** and **4b** respectively. In dimeric **4c**, the magnetic moment of 8.04 BM is consistent with two non-interacting high spin manganese(II) centres (using $\mu^2 = \sum \mu_i^2$, where μ_i is the magnetic moment of the individual metal centres). The FAB mass spectra of **4a** and **4b** give either molecular ion peaks and/or fragmentation peaks

corresponding to the loss of a chloride ion from the molecular ion peak along with minor peaks that can be ascribed to dimeric species. In the FAB mass spectrum of **4c**, a [M – Cl]⁺ peak is observed along with a peak corresponding to the loss of a chloride ion from a monomeric species.

Clearly, the steric properties of **L3** play a key role on the ability for the ligand to bind in a tetradentate fashion. While the presence of a single *ortho*-methyl group (**L3a**) on the aryl-substituted amine arm leads to efficient coordination (**3**), the introduction of a second methyl group at the *ortho* position (**L3b**) results in either a loosely bound amine (**4b**) or in decoordination of the amine altogether (**4c**). Indeed we have previously suggested that the lability of arylamine arm could be a factor involved in *mer/fac* interconversions that are evident for [(*N*-picolylen)FeCl₂] in solution.⁸

To probe the solution state properties of **3** and **4**, the ¹H NMR spectra of the iron(II) complexes **3b** and **4b** were recorded. The spectra are typical of high spin ferrous species containing broad paramagnetically shifted resonances. By consideration of the chemical shifts, relaxation times and comparison with the spectra of [(tpa)FeCl₂] (tpa = tripicolylamine),¹⁹ [(dpa)FeCl(μ-Cl)]₂,²⁰ [{(2,6-Me₂C₆H₃)NHCH₂CH₂}{(2-C₅H₄N)CH₂}NH]-FeCl₂⁸ and related polypyridyl iron complexes,¹⁶ assignment of the peaks has been tentatively made (see Table 6). The Py–H_α of the coordinated pyridyl arms in **3b** and **4b** are characteristically the furthest downfield at δ = 139.1 and 120.2 with low values for T₁ (0.5 ms and 0.4 ms), respectively. The Py–H_{β/β'} and Py–H_γ appear at δ = 53.0 (T₁ = 11.7 ms), 45.5 (T₁ = 10.0 ms) and 27.6 (T₁ = 37.9 ms) for **3b**, whilst for **4b** they are found at δ = 51.9 (T₁ = 11.4 ms), 51.1 (T₁ = 9.3 ms) and 19.3 (T₁ = 26.3 ms). All four sets of methylene protons are assigned for **4b** at δ = 73.5 (T₁ = 1.3 ms), *ca.* 72 (shoulder of δ = 73.5), 28.7 (T₁ = 1.0 ms) and 12.2 (T₁ = 1.7 ms). In contrast, for **3b** only one very broad methylene peak is assigned at *ca.* δ = 46. In each case the aromatic peaks are shifted further downfield than their free ligand counterparts (**L3a** and **L3b**) and in **3b** they are shifted more so than **4b**.

Given the similarity in chemical shift for the picolyl protons in **4b** with [(dpa)FeCl(μ-Cl)]₂²⁰ (see Table 6), in which the dpa binds as a tridentate ligand, it would seem reasonable to suggest that the aryl amine arm in **4b** is pendant in solution. Nevertheless, some degree of interaction seems likely and sufficient enough to cause the aromatic protons to be paramagnetically shifted in **4b**.

Table 6 ^1H NMR chemical shifts (δ) and relaxation times (T_1) for complexes **3b**, **4b** (in acetonitrile- d_3 at room temperature) and related complexes

Compound	Py- H_a	Py- $H_{\beta/\gamma}$	Py- H_γ	CH_2	Ar- H	Ar- Me	Ref.
$[(\text{dpa})\text{FeCl}(\mu\text{-Cl})_2]$	116.5 (0.4)	54.7 (10.1), 51.8 (9.1)	7.8	70.8 (1.1)	Not applicable	Not applicable	20
$[(\text{tpa})\text{FeCl}_2]$	130.0 (0.2)	51.3 (6.95), 50.5 (4.18), 46.4 (4.63), 45.8 (3.79)	25.2 (11.83), 24.8 (6.40)	42 (very broad), 0.5 (0.78)	Not applicable	Not applicable	19
$[(2,6\text{-Me}_2\text{Ph})\text{NHCH}_2\text{CH}_2\text{-}\{(2\text{-C}_5\text{H}_4\text{N})\text{CH}_2\text{-NH}\}\text{FeCl}_2]$	130.4	58.8 (16.4), 57.4 (14.6)	15.8 (37.1)	104.9 (0.96), 80.9 (0.73), 62.9 (0.90)	12.3 (34.2, Ar- H_m), -5.4 (Ar- H_p)	6.6 (2.0, Ar- Me_e)	8
	139.1 (0.5)	53.0 (11.7), 45.5 (10.0)	27.6 (37.9)	46 (very broad)	21.9 (Ar- H_m), 15.1 (29.6, Ar- H_o)	19.1 (2.0, Ar- Me_e), 16.1 (Ar- Me_o)	This work
	120.2 (0.4)	51.9 (11.4), 51.1 (9.3),	19.3 (26.3)	73.5 (1.3), ca. 72.0, 28.7 (1.0), 12.2 (1.7)	14.5 (31.9, Ar- H_m), 0.62 (Ar- H_p)	9.7 (3.1, Ar- Me_o)	This work

In summary, the *N*-picolylen ligand frame developed in our earlier study⁸ has been shown to be amenable to functionalisation at the central nitrogen atom with methyl (**L1**), 4-vinylbenzyl (**L2**) and 2-picolylyl (**L3**) derivatives accessible. While **L1** and **L2** act as tridentate ligands, the introduction of a 2-picolylyl group in **L3** has allowed access to a tripodal ligand that can bind to a range of paramagnetic transition metal chlorides as either a tridentate or tetradentate ligand; the denticity being dependent on the steric bulk in the *ortho*-positions of the aryl groups. The role of these systems as precatalysts for olefin polymerisation and other catalytic applications is currently being probed as is the potential immobilisation of **L2** (and its complexes) and will be published in due course.

3 Experimental

3.1 General

All reactions were carried out under an atmosphere of dry, oxygen-free nitrogen, using standard Schlenk techniques or in a nitrogen purged glove box. Solvents were distilled under nitrogen from appropriate drying agents and degassed prior to use.²¹ The infrared spectra were recorded as Nujol mulls between 0.5 mm NaCl plates on a Perkin Elmer 1600 series. The ES and the FAB mass spectra were recorded using a micromass Quattro LC mass spectrometer and a Kratos Concept spectrometer with methanol or NBA as the matrix, respectively. ^1H and ^{13}C NMR spectra were recorded on a Bruker ARX spectrometer (250 or 300 or 400 MHz) at ambient temperature; chemical shifts (ppm) are referred to the residual protic solvent peaks; relaxation times (T_1) are in seconds. Magnetic susceptibility studies were performed using an Evans Balance (Johnson Matthey) at room temperature. The magnetic moment was calculated following standard methods²² and corrections for underlying diamagnetism were applied to data.²³ Elemental analyses were performed at the Department of Chemistry, University of North London by Dr S. Boyer.

The reagents, methyl iodide, 4-vinylbenzyl chloride, 2-picolylyl chloride hydrochloride, sodium *t*-butoxide, the aryl halides and the metal dichlorides were purchased from Aldrich Chemical Co. and used without further purification. *rac*-BINAP was purchased from Strem Chemical Co. The compounds, $\text{FeCl}_2(\text{THF})_{1.5}$,²⁴ $\text{Pd}_2(\text{dba})_3$,²⁵ *N*-tosylaziridine,¹² *N,N*-bis(2-picolylyl)amine (dpa),¹⁰ and $(\text{ArNHCH}_2\text{CH}_2)\{(2\text{-C}_5\text{H}_4\text{N})\text{CH}_2\}\text{NH}$ (Ar = 2,4,6- $\text{Me}_3\text{C}_6\text{H}_2$, 2,4- $\text{Me}_2\text{C}_6\text{H}_3$, 2,6- $\text{Me}_2\text{C}_6\text{H}_3$)⁸ were prepared according to previously reported procedures. All other chemicals were obtained commercially and used without further purification.

3.2 Synthesis of *N,N*-dipicolylethylenediamine (dpea)

Prepared via two-step procedure.

(a) (*N*-tosyl-2-aminoethyl)bis(2-picolylyl)amine. To a 3-necked round bottom flask equipped with a reflux condenser, dropping funnel and a magnetic stirrer was added dpa (19.900 g, 100 mmol) dissolved in acetonitrile (250 ml). The yellow solution was brought to reflux and *N*-tosylaziridine (19.700 g, 100 mmol) in acetonitrile (200 ml) was added dropwise over 1 h, to give a dark red solution, which was heated to reflux for an additional 5 h. The dark red solution was concentrated and dried under reduced pressure overnight to give (*N*-tosyl-2-aminoethyl)bis(2-picolylyl)amine as a dark red oil. Yield: 99% (39.204 g, 99.0 mmol). ES mass spectrum: m/z 397 $[\text{M} + \text{H}]^+$. ^1H NMR (CDCl_3 , 250 MHz): δ 2.36 (s, 3H, Me), 2.77 (t, 2H, $^3J(\text{HH})$ 5.3, CH_2), 3.03 (t, 2H, CH_2), 3.76 (s, 4H, PyCH_2), 7.1–7.2 (m, 6H, Ar- H and Py- H), 7.57 (d, 2H, $^3J(\text{HH})$ 6.0, Py- H), 7.71 (d, 2H, $^3J(\text{HH})$ 8.0, Py- H) and 8.58 (d, 2H, $^3J(\text{HH})$ 4.6, Py- H).

(b) *N,N*-dipicolylethylenediamine (dpea). To (*N*-tosyl-2-aminoethyl)bis(2-picolylyl)amine (39.20 g, 99.0 mmol) was added concentrated H_2SO_4 (300 ml). The dark red solution was stirred and heated to 130 °C. After 3 days, the reaction mixture

was cooled in an ice bath and diethyl ether (4000 ml) and absolute ethanol (3000 ml) added dropwise to give a dark brown precipitate. *Caution! The brown precipitate is hygroscopic.* The brown precipitate was filtered and immediately dissolved in saturated NaOH. The organic layer was extracted with chloroform (3 × 200 ml) and the organic phases combined and dried over MgSO₄. Following filtration, the solution was concentrated to give (H₂NCH₂CH₂){(2-C₅H₄N)CH₂}₂N as a red oil. Yield: 73% (17.45 g, 72.0 mmol). ES mass spectrum: *m/z* 243 [M + H]⁺. IR (cm⁻¹) 3360 (N–H), 1590 (C=N_{pyridine}). ¹H NMR (CDCl₃, 250 MHz): δ 1.65 (s br, 2H, NH₂), 2.67 (t, 2H, ³J(HH) 5.7, CH₂), 2.80 (t, 2H, CH₂), 3.85 (s, 4H, PyCH₂), 7.14 (dd, 2H, ³J(HH) 7.5, 5.0, Py–H), 7.49 (d, 2H, ³J(HH) 7.8, Py–H), 7.65 (dd, 2H, ³J(HH) 7.5, 6.9, Py–H) and 8.53 (d, 2H, ³J(HH) 5.0, Py–H). ¹³C NMR (CDCl₃, 63 MHz, ¹H composite pulse decoupled): δ 39.9 (s, CH₂), 57.8 (s, CH₂), 61.1 (s, PyCH₂), 122.4 (s, Py–CH), 123.4 (s, Py–CH), 136.8 (s, Py–CH), 149.4 (s, Py–CH) and 160.0 (s, Py–C).

3.3 Synthesis of {(2,4,6-Me₃C₆H₂)NHCH₂CH₂}{(2-C₅H₄N)CH₂}₂NMe (L1)

An oven-dried Schlenk flask equipped with a magnetic stir bar was evacuated and backfilled with nitrogen. The flask was charged with {(2,4,6-Me₃C₆H₂)NHCH₂CH₂}{(2-C₅H₄N)CH₂}₂NH (0.200 g, 0.74 mmol), K₂CO₃ (0.154 g, 1.12 mmol) in MeCN (40 ml) and cooled to –10 °C. MeI (0.05 ml, 0.82 mmol) in MeCN (40 ml) was added dropwise over the course of 1 h before warming of the reaction mixture to room temperature and stirring for an additional 1 h. The reaction mixture was filtered and the solvent removed under reduced pressure to afford an oily residue. The residue was dissolved in dichloromethane (30 ml) and washed with water (3 × 30 ml). The organic layer was separated, dried over MgSO₄ and the volatiles removed under reduced pressure to give a brown oil. The crude product was purified *via* alumina column chromatography (active neutral Brockmann grade 1) employing ethyl acetate and hexane (1 : 3) as the eluting solvent mixture to give {(2,4,6-Me₃C₆H₂)NHCH₂CH₂}{(2-C₅H₄N)CH₂}₂NMe (L1) as a yellow oil. Yield: 63% (0.132 g, 0.47 mmol). ES mass spectrum, *m/z* 284 [M + H]⁺. IR (cm⁻¹) 3356 (N–H). ¹H NMR (CDCl₃, 300 MHz): δ 2.13 (s, 3H, Me_p), 2.18 (s, 6H, Me_o), 2.20 (s, 3H, N–Me), 2.61 (t, 2H, ³J(HH) 6.0, CH₂), 3.00 (t, 2H, CH₂), 3.65 (s, 2H, PyCH₂), 6.72 (s, 2H, Ar–H), 7.07 (m, 1H, Py–H), 7.39 (d, 1H, ³J(HH) 7.6, Py–H), 7.67 (dt, 1H, ³J(HH) 7.5, ⁴J(HH) 1.6, Py–H) and 8.46 (d, 1H, ³J(HH) 7.5, Py–H). ¹³C NMR (CDCl₃, 75 MHz, ¹H composite pulse decoupled): δ 17.5 (s, Me_o), 19.5 (s, Me_p), 40.94 (s, N–Me), 44.9 (s, CH₂), 56.7 (s, CH₂), 63.3 (s, Py–CH₂), 121.0 (s, Py–C), 121.8 (s, Py–C), 127.9 (s, Ar–C), 128.4 (s, Ar–C), 129.6 (s, Ar–C), 135.4 (s, Py–C), 143.0 (s, Ar–C), 148.0 (s, Py–C) and 158.3 (s, Py–C).

3.4 Synthesis of {(2,6-Me₂C₆H₃)NHCH₂CH₂}{(2-C₅H₄N)CH₂}₂N(CH₂C₆H₄CH=CH₂) (L2)

An oven-dried Schlenk flask equipped with a magnetic stir bar was evacuated and backfilled with nitrogen. The flask was charged with {(2,6-Me₂C₆H₃)NHCH₂CH₂}{(2-C₅H₄N)CH₂}₂NH (0.667 g, 2.62 mmol), 4-vinylbenzyl chloride (0.600 g, 0.55 ml, 3.93 mmol), K₂CO₃ (1.08 g, 7.86 mmol) and acetonitrile (60 ml). The reaction mixture was heated to 80 °C and stirred at this temperature for a period of 3 days. After cooling to room temperature, the contents were filtered and the solvent removed under reduced pressure to afford an oily residue. The residue was dissolved in dichloromethane (40 ml) and washed with water (3 × 40 ml). The organic layer was separated, dried over MgSO₄ and the volatiles removed under reduced pressure to give a brown oil. The crude product was purified *via* alumina column chromatography (active neutral Brockmann grade 1) employing ethyl acetate and hexane (1 : 4) as the elut-

ing solvent mixture to give {(2,6-Me₂C₆H₃)NHCH₂CH₂}{(2-C₅H₄N)CH₂}₂N(CH₂C₆H₄CH=CH₂) (L2) as a yellow oil. Yield: 41% (0.401 g, 1.08 mmol). ES mass spectrum, *m/z* 372 [M + H]⁺. IR (cm⁻¹) 3361 (N–H), 1629 (C=C). ¹H NMR (CDCl₃, 300 MHz): δ 2.15 (s, 6H, Me_o), 2.70 (t, 2H, ³J(HH) 6.2, CH₂), 3.07 (t, 2H, CH₂), 3.62 (s, 2H, Py–CH₂), 3.73 (s, 2H, Styr–CH₂), 5.15 (d, 1H, ³J(HH) 11.0, vinyl–H), 5.65 (d, 1H, ³J(HH) 17.0, vinyl–H), 6.6–6.7 (m, 2H, Ar–H and vinyl–H), 6.87 (d, 2H, ³J(HH) 7.6, Ar–H), 7.07 (m, 1H, Py–H), 7.2–7.3 (m, 4H, Ar–H), 7.40 (d, 1H, ³J(HH) 7.9, Py–CH), 7.57 (dt, 1H, ³J(HH) 7.6, ⁴J(HH) 1.8, Py–H) and 8.45 (d, 1H, ³J(HH) 6.0, PyCH). ¹³C NMR (CDCl₃, 75 MHz, ¹H composite pulse decoupled): δ 17.8 (s, Me_o), 44.7 (s, CH₂), 53.3 (s, CH₂), 57.4 (s, Py–CH₂), 58.9 (s, Styr–CH₂), 112.5 (s, vinyl–C), 120.0 (s, Py–C), 121.0 (s, Py–C), 122.0 (s, Ar–C), 125.2 (s, Ar–C), 127.3 (s, Ar–C), 127.8 (s, Ar–C), 128.2 (s, Ar–C), 135.4 (s, Py–C), 135.5 (s, vinyl–C), 137.3 (s, Ar–C), 145.5 (s, Ar–C), 147.9 (s, Py–C) and 158.5 (s, Py–C).

3.5 Synthesis of {(Ar)NHCH₂CH₂}{(2-C₅H₄N)CH₂}₂N (L3)

(a) L3a, Ar = 2,4-Me₂C₆H₃. An oven-dried Schlenk flask equipped with a magnetic stir bar was evacuated and backfilled with nitrogen. The flask was charged with {(2,4-Me₂C₆H₃)NHCH₂CH₂}{(2-C₅H₄N)CH₂}₂NH (1.00 g, 3.92 mmol), 2-picolyl chloride hydrochloride (0.965 g, 5.88 mmol), K₂CO₃ (1.628 g, 11.8 mmol) and acetonitrile (80 ml). The reaction mixture was heated to 55 °C and stirred for a period of 3 days. After cooling to room temperature, the contents were filtered and the solvent removed under reduced pressure to afford an oily residue. The residue was dissolved in dichloromethane (50 ml) and washed with water (3 × 50 ml). The organic layer was separated, dried over MgSO₄ and the volatiles removed under reduced pressure to give a brown oil. The crude product was purified *via* alumina column chromatography (active neutral Brockmann grade 1) employing ethyl acetate and hexane (1 : 4) as the eluting solvent mixture to give {(2,4-Me₂C₆H₃)NHCH₂CH₂}{(2-C₅H₄N)CH₂}₂N (L3a) as a yellow oil. Yield: 38% (0.515 g, 1.49 mmol). ES mass spectrum, *m/z* 347 [M + H]⁺. IR (cm⁻¹) 3331 (N–H). ¹H NMR (CDCl₃, 250 MHz): δ 2.10 (s, 3H, Me_p), 2.13 (s, 3H, Me_o), 2.83 (t, 2H, ³J(HH) 6.0, CH₂), 3.12 (t, 2H, CH₂), 3.79 (s, 4H, Py–CH₂), 6.35 (d, 1H, ³J(HH) 8.5, Ar–H), 6.79 (m, 2H, Ar–H), 7.05 (t, 2H, ³J(HH) 7.6, Py–H), 7.37 (d, 2H, ³J(HH) 7.8, Py–H), 7.53 (dt, 2H, ³J(HH) 7.5, ⁴J(HH) 1.6, Py–H) and 8.45 (d, 2H, ³J(HH) 4.8, Py–H). ¹³C NMR (CDCl₃, 63 MHz, ¹H composite pulse decoupled): δ 17.9 (s, Me_o), 20.7 (s, Me_p), 41.7 (s, CH₂), 53.1 (s, CH₂), 60.6 (s, PyCH₂), 110.3 (s, Ar–C), 122.5 (s, Ar–C), 122.5 (s, Py–C), 123.4 (s, Py–C), 126.1 (s, Ar–C), 127.7 (s, Ar–C), 131.2 (s, Ar–C), 136.8 (s, Py–C), 144.7 (s, Ar–C), 149.6 (s, Py–C) and 159.8 (s, Py–C).

(b) L3b, Ar = 2,6-Me₂C₆H₃. Using the same procedure and molar quantities of reagents as above in 3.5(a), employing {(2,6-Me₂C₆H₃)NHCH₂CH₂}{(2-C₅H₄N)CH₂}₂NH (1.00 g, 3.92 mmol), 2-picolyl chloride hydrochloride (0.965 g, 5.88 mmol), K₂CO₃ (1.628 g, 11.8 mmol) and acetonitrile (80 ml), afforded {(2,6-Me₂C₆H₃)NHCH₂CH₂}{(2-C₅H₄N)CH₂}₂N (L3b) as a yellow oil. Yield: 35% (0.48 g, 1.4 mmol). ES mass spectrum, *m/z* 347 [M + H]⁺. IR (cm⁻¹) 3354 (N–H). ¹H NMR (CDCl₃, 250 MHz): δ 2.20 (s, 6H, Me_o), 2.80 (t, 2H, ³J(HH) 6.0, CH₂), 3.10 (t, 2H, CH₂), 3.80 (s, 4H, Py–CH₂), 6.68 (m, 1H, Ar–H), 6.87 (d, 2H, ³J(HH) 7.4, Ar–H), 7.07 (m, 2H, Py–H), 7.42 (d, 2H, ³J(HH) 8.1, Py–H), 7.60 (dt, 2H, ³J(HH) 6.0, ⁴J(HH) 1.1, Py–H) and 8.47 (dd, 2H, ³J(HH) 4.8, ⁴J(HH) 1.6, Py–H). ¹³C NMR (CDCl₃, 63 MHz, ¹H composite pulse decoupled): δ 19.2 (s, Me_o), 46.2 (s, CH₂), 55.0 (s, CH₂), 60.8 (s, Py–CH₂), 121.5 (s, Ar–C), 122.5 (s, Py–C), 123.5 (s, Py–C), 129.2 (s, Ar–C), 136.8 (s, Py–C), 138.9 (s, Ar–C), 147.0 (s, Ar–C), 149.6 (s, Py–C) and 159.7 (s, Py–C).

3.6 Alternative synthesis of $\{(Ar)NHCH_2CH_2\}\{(2-C_5H_4N)CH_2\}_2N$ (**L3**)

(a) **L3a**, Ar = 2,4-Me₂C₆H₃. An oven-dried Schlenk flask equipped with a magnetic stir bar was evacuated and backfilled with nitrogen. The flask was charged with dpea (3.68 g, 15.2 mmol), 2,4-dimethylphenyl bromide (2.5 ml, 3.36 g, 18.2 mmol), Pd₂(dba)₃ (0.028 g, 0.030 mmol), *rac*-BINAP (0.061 g, 0.10 mmol), NaOBu^t (1.90 g, 20 mmol) and toluene (30 ml). The reaction mixture was heated to reflux and stirred for 4 days. After cooling to room temperature, the solvent was removed under reduced pressure to afford an oil residue. The residue was dissolved in diethyl ether, washed with water and saturated NaCl solution. The organic layer was separated and dried over MgSO₄. The volatiles were removed under reduced pressure and the residue left under vacuum at 50 °C for 24 h to give $\{(2,4-Me_2C_6H_3)NHCH_2CH_2\}\{(2-C_5H_4N)CH_2\}_2N$ (**L3a**) as a viscous brown oil. Yield: 74% (4.237 g, 12.25 mmol). The spectroscopic data were as described in 3.5(a).

(b) **L3b**, Ar = 2,6-Me₂C₆H₃. Using an analogous route to that outlined in 3.6(a) employing dpea (4.00 g, 16.5 mmol), 2,6-dimethylphenyl bromide (2.42 ml, 3.36 g, 18.2 mmol), Pd₂(dba)₃ (0.032 g, 0.034 mmol), *rac*-BINAP (0.064 g, 0.11 mmol), NaOBu^t (1.982 g, 21.0 mmol) and toluene (30 ml) gave $\{(2,6-Me_2C_6H_3)NHCH_2CH_2\}\{(2-C_5H_4N)CH_2\}_2N$ (**L3b**) as a viscous oil. Yield: 85% (4.864 g, 14.0 mmol). The spectroscopic data were as described in 3.5(b).

3.7 Synthesis of $\{((2,4,6-Me_3C_6H_2)NHCH_2CH_2)\{(2-C_5H_4N)CH_2\}_2NMe\}MCl_2$ (**1**)

(a) **1a**, M = Co. An oven-dried Schlenk flask equipped with a magnetic stir bar was evacuated and backfilled with nitrogen. The flask was charged with CoCl₂·6H₂O (0.066 g, 0.28 mmol) in THF (5 ml) at room temperature and **L1** (0.080 g, 0.28 mmol) was introduced to form a purple solution. After being stirred at room temperature for 24 h, the reaction mixture was concentrated and hexane added to induce precipitation of [(**L1**)CoCl₂] (**1a**) as a purple solid. The suspension was stirred overnight, filtered, washed with hexane (2 × 30 ml) and dried under reduced pressure. Recrystallisation from hot acetonitrile gave purple crystals of **1a** suitable for single crystal X-ray structure determination. Yield: 72% (0.087 g, 0.21 mmol).

(b) **1b**, M = Fe. Using an analogous procedure and molar ratios of reagents to that described above in 3.7(a) employing **L1** (0.080 g, 0.28 mmol) and FeCl₂(THF)_{1.5} (0.066 g, 0.28 mmol), gave [(**L1**)FeCl₂] (**1b**) as a pale yellow powder. Yield: 66% (0.076 g, 0.19 mmol).

3.8 Synthesis of $\{((2,6-Me_2C_6H_3)NHCH_2CH_2)\{(2-C_5H_4N)CH_2\}_2N(CH_2C_6H_4CH=CH_2)\}MCl_2$ (**2**)

(a) **2a**, M = Co. An oven-dried Schlenk flask equipped with a magnetic stir bar was evacuated and backfilled with nitrogen. The flask was charged with CoCl₂·6H₂O (0.022 g, 0.09 mmol) in THF (5 ml) at room temperature and **L2** (0.033 g, 0.09 mmol) was introduced to form a blue solution. After being stirred at room temperature for 24 h, the reaction mixture was concentrated and hexane added to induce precipitation of [(**L2**)CoCl₂] (**2a**) as a blue solid. The suspension was stirred overnight, filtered, washed with hexane (2 × 30 ml) and dried under reduced pressure. Yield: 65% (0.030 g, 0.06 mmol). IR (cm⁻¹), 1628 (C=C).

(b) **2b**, M = Fe. Using an analogous procedure to that described above in 3.8(a) employing **L2** (0.056 g, 0.15 mmol) and FeCl₂(THF)_{1.5} (0.035 g, 0.15 mmol), gave [(**L2**)FeCl₂] (**2b**) as a pale yellow powder. Yield: 63% (0.047 g, 0.09 mmol). IR (cm⁻¹), 1626 (C=C).

3.9 Synthesis of $\{((2,4-Me_2C_6H_3)NHCH_2CH_2)\{(2-C_5H_4N)CH_2\}_2N\}MCl_2$ (**3**)

(a) **3a**, M = Co. An oven-dried Schlenk flask equipped with a magnetic stir bar was evacuated and backfilled with nitrogen. The flask was charged with CoCl₂ (0.020 g, 0.15 mmol) in *n*-BuOH (5 ml) and the reaction stirred at 90 °C until dissolution. **L3a** (0.052 g, 0.15 mmol) in *n*-BuOH (2 ml) was added and the reaction mixture stirred at 90 °C for 20 min. Following concentration of the reaction mixture, hexane was added to induce precipitation of the product. The suspension was stirred overnight, filtered, washed with hexane (2 × 30 ml) and dried under reduced pressure to afford [(**L3a**)CoCl₂] (**3a**) as a pale blue solid. Yield: 65% (0.046 g, 0.10 mmol).

(b) **3b**, M = Fe. Using an analogous procedure to that described above in 3.9(a) employing **L3a** (0.138 g, 0.40 mmol) and FeCl₂ (0.050 g, 0.40 mmol), gave [(**L3a**)FeCl₂] (**3b**) as a yellow powder. Recrystallisation from a hot acetonitrile solution gave **3b** as yellow crystals. Yield: 79% (0.151 g, 0.32 mmol).

(c) **3c**, M = Mn. Using an analogous procedure to that described above in 3.9(a) employing **L3a** (0.194 g, 0.56 mmol) and MnCl₂ (0.070 g, 0.56 mmol), gave [(**L3a**)MnCl₂] (**3c**) as a white powder. Layering of an acetonitrile solution with hexane gave **3c** as clear crystals. Yield: 65% (0.170 g, 0.36 mmol).

3.10 Synthesis of $\{((2,6-Me_2C_6H_3)NHCH_2CH_2)\{(2-C_5H_4N)CH_2\}_2N\}MCl_2$ (**4**)

(a) **4a**, M = Co, *n* = 1. An oven-dried Schlenk flask equipped with a magnetic stir bar was evacuated and backfilled with nitrogen. The flask was charged with CoCl₂ (0.022 g, 0.17 mmol) in *n*-BuOH (5 ml) and the reaction stirred at 90 °C until dissolution of the metal salt. **L3b** (0.059 g, 0.17 mmol) in *n*-BuOH (2 ml) was added and the reaction mixture stirred at 90 °C for a further 20 min. Following concentration of the reaction mixture, hexane was added to induce precipitation of the product. The suspension was stirred overnight, filtered, washed with hexane (2 × 30 ml) and dried under reduced pressure to afford [(**L3b**)CoCl₂] (**4a**) as a pale blue solid. Yield: 68% (0.055 g, 0.16 mmol).

(b) **4b**, M = Fe, *n* = 1. Using an analogous procedure and molar ratios to that described in 3.10(a) employing **L3b** (0.059 g, 0.17 mmol) and FeCl₂ (0.022 g, 0.17 mmol), gave [(**L3b**)FeCl₂] (**4b**) as a yellow powder. Recrystallisation from a hot acetonitrile solution gave **4b** as yellow crystals. Yield: 65% (0.052 g, 0.11 mmol).

(c) **4c**, M = Mn, *n* = 2. Using an analogous procedure to that described in 3.10(a) using MnCl₂ (0.076 g, 0.60 mmol) and **L3b** (0.208 g, 0.60 mmol) gave [(**L3b**)MnCl(μ-Cl)]₂ (**4c**) as a white solid. Layering of an acetonitrile solution of **4c** with hexane gave **4c** as clear crystals. Yield: 71% (0.198 g, 0.21 mmol).

3.11 Crystallography

Data for **1a**, **3b**-MeCN, **3c**-MeCN, **4b**-MeCN and **4c** were collected on a Bruker APEX 2000 CCD diffractometer. Details of data collection, refinement and crystal data are listed in Table 7. The data were corrected for Lorentz and polarisation effects and empirical absorption corrections applied. Structure solution by Patterson methods and structure refinement on *F*² employed SHELXTL version 6.10.^{26,27} Hydrogen atoms were included in calculated positions (C–H = 0.96 Å) riding on the bonded atom with isotropic displacement parameters set to 1.5 *U*_{eq}(C) for methyl H atoms and 1.2 *U*_{eq}(C) for all other H atoms. All non H atoms were refined with anisotropic displacement parameters.

CCDC reference numbers 270047–270051.

See <http://dx.doi.org/10.1039/b505763a> for crystallographic data in CIF or other electronic format.

Table 7 Crystallographic and data processing parameters for complexes 1a, 3b-MeCN, 3c-MeCN, 4b-MeCN and 4c^a

Complex	1a	3b-MeCN	3c-MeCN	4b-MeCN	4c
Formula	C ₁₈ H ₂₅ Cl ₂ CoN ₅	C ₂₂ H ₃₆ Cl ₂ N ₄ Fe·CH ₃ CN	C ₂₂ H ₃₆ Cl ₂ N ₄ Mn·CH ₃ CN	C ₂₂ H ₃₆ Cl ₂ N ₄ Fe·CH ₃ CN	C ₄₄ H ₃₂ Cl ₄ Mn ₂ N ₈
<i>M</i>	413.24	514.27	513.36	514.27	944.62
Crystal size/mm	0.30 × 0.19 × 0.06	0.47 × 0.21 × 0.04	0.34 × 0.30 × 0.04	0.32 × 0.25 × 0.08	0.26 × 0.21 × 0.05
Temperature/K	150(2)	150(2)	150(2)	150(2)	150(2)
Crystal system	Monoclinic	Monoclinic	Monoclinic	Triclinic	Monoclinic
Space group	<i>P</i> 2 ₁ / <i>c</i>	<i>P</i> 2 ₁ / <i>c</i>	<i>P</i> 2 ₁ / <i>c</i>	<i>P</i> $\bar{1}$	<i>P</i> 2 ₁ / <i>n</i>
Lattice parameters					
<i>a</i> /Å	15.410(3)	19.206(4)	19.337(3)	7.5084(13)	12.080(2)
<i>b</i> /Å	7.4772(14)	14.800(3)	14.843(2)	12.873(2)	14.978(3)
<i>c</i> /Å	16.863(3)	17.270(4)	17.351(3)	12.978(2)	13.642(3)
<i>a</i> /°	90	90	90	82.257(3)	90
<i>β</i> /°	94.761(3)	99.752(4)	99.618(3)	86.705(3)	116.103(3)
<i>γ</i> /°	90	90	90	83.201(3)	90
<i>U</i> /Å ³	1936.2(6)	4838.1(18)	4910.0(13)	1233.1(4)	2216.5(7)
<i>Z</i>	4	8	8	2	2
<i>D_c</i> /Mg m ⁻³	1.418	1.412	1.389	1.385	1.415
<i>F</i> (000)	860	2144	2136	536	980
<i>μ</i> (Mo-K _α)/mm ⁻¹	1.167	0.866	0.777	0.850	0.852
Reflections collected	13964	26576	34315	9702	15715
Independent reflections	3785	8503	8554	4770	3891
<i>R</i> _{int}	0.0809	0.1551	0.0788	0.0231	0.0352
Parameters/restraints	221/0	584/0	583/0	292/0	264/0
Final <i>R</i> indices					
<i>I</i> > 2σ(<i>I</i>)	<i>R</i> ₁ = 0.0689, <i>wR</i> ₂ = 0.1574	<i>R</i> ₁ = 0.0787, <i>wR</i> ₂ = 0.1608	<i>R</i> ₁ = 0.1020, <i>wR</i> ₂ = 0.2577	<i>R</i> ₁ = 0.0349, <i>wR</i> ₂ = 0.0849	<i>R</i> ₁ = 0.0306, <i>wR</i> ₂ = 0.0693
All data	<i>R</i> ₁ = 0.1024, <i>wR</i> ₂ = 0.1751	<i>R</i> ₁ = 0.1670, <i>wR</i> ₂ = 0.1970	<i>R</i> ₁ = 0.1256, <i>wR</i> ₂ = 0.2695	<i>R</i> ₁ = 0.0407, <i>wR</i> ₂ = 0.0883	<i>R</i> ₁ = 0.0389, <i>wR</i> ₂ = 0.0719
Goodness of fit on <i>F</i> ² (all data)	1.039	0.882	1.099	1.031	1.012

^a Data in common: graphite-monochromated Mo-K_α radiation, λ = 0.71073 Å; *R*₁ = Σ||*F*_o|| - |*F*_c||/Σ|*F*_o||, *wR*₂ = [Σw(*F*_o² - *F*_c²)/Σw(*F*_o²)]^{1/2}, *w*⁻¹ = [σ²(*F*_o²) + (*aP*)²]/3, where *a* is a constant adjusted by the program; goodness of fit = [Σ(*F*_o² - *F*_c²)/2(*n* - *p*)]^{1/2}, where *n* is the number of reflections and *p* the number of parameters.

Acknowledgements

We thank the EPSRC (to CJD) and ExxonMobil (to CJD) for financial assistance. Financial and equipment support from the Department of Chemistry at the University of Leicester and the Royal Society are gratefully acknowledged. Johnson Matthey PLC are thanked for their loan of palladium chloride.

References

- (a) L.-C. Liang, R. R. Schrock, W. M. Davis and D. H. McConville, *J. Am. Chem. Soc.*, 1999, **121**, 5797; (b) R. R. Schrock, A. L. Casado, J. T. Goodman, L.-C. Liang, P. J. Bonitatebus, Jr. and W. M. Davis, *Organometallics*, 2000, **19**, 5325; (c) R. R. Schrock, P. J. Bonitatebus, Jr. and Y. Schrodi, *Organometallics*, 2001, **20**, 1056; (d) Y. Schrodi, R. R. Schrock and P. J. Bonitatebus, Jr., *Organometallics*, 2001, **20**, 3560.
- (a) F. Guérin, D. H. McConville and J. J. Vittal, *Organometallics*, 1996, **15**, 5586; (b) F. Guérin, D. H. McConville and N. C. Payne, *Organometallics*, 1996, **15**, 5085; (c) F. Guérin, D. H. McConville, J. J. Vittal and G. A. P. Yap, *Organometallics*, 1998, **17**, 5172; (d) F. Guérin, D. H. McConville and J. J. Vittal, *Organometallics*, 1997, **16**, 1491.
- D. Reardon, F. Conan, S. Gambarotta, G. Yap and Q. Wang, *J. Am. Chem. Soc.*, 1999, **121**, 9318.
- M. A. Esteruelas, A. M. Lopez, L. Mendez, M. Olivan and E. Onate, *Organometallics*, 2003, **22**, 395.
- (a) B. L. Small and M. Brookhart, *J. Am. Chem. Soc.*, 1998, **120**, 7143; (b) B. L. Small, M. Brookhart and A. M. A. Bennett, *J. Am. Chem. Soc.*, 1998, **120**, 4049; (c) A. M. A. Bennett, (Dupont) WO 98/27124, 1998, [*Chem. Abstr.*, 1998, **129**, 122973x].
- (a) G. J. P. Britovsek, V. C. Gibson, B. S. Kimberley, P. J. Maddox, S. J. McTavish, G. A. Solan, A. J. P. White and D. J. Williams, *Chem Commun.*, 1998, 849; (b) G. J. P. Britovsek, M. Bruce, V. C. Gibson, B. S. Kimberley, P. J. Maddox, S. Mastroianni, S. J. McTavish, C. Redshaw, G. A. Solan, S. Strömberg, A. J. P. White and D. J. Williams, *J. Am. Chem. Soc.*, 1999, **121**, 8728; (c) G. J. P. Britovsek, B. A. Dorer, V. C. Gibson, B. S. Kimberley and G. A. Solan, WO patent, 99/12981 (BP Chemicals Ltd), [*Chem. Abstr.*, 1999, **130**, 252793].
- V. C. Gibson and S. K. Spitzmesser, *Chem. Rev.*, 2003, **103**, 283.
- R. Cowdell, C. J. Davies, S. J. Hilton, J.-D. Maréchal, G. A. Solan, O. Thomas and J. Fawcett, *Dalton Trans.*, 2004, 3231.
- For examples of 4-vinylbenzyl side arms see: (a) N. J. Long, D. G. Parker, P. R. Speyer, A. J. P. White and D. J. Williams, *J. Chem. Soc., Perkin Trans. 1*, 1999, 1621; (b) Q. Lu, A. Singh, J. R. Deschamps and E. L. Chang, *Inorg. Chim. Acta*, 2000, **309**, 82; (c) H. Chen, M. M. Olmstead, R. L. Albright, J. Devenyi and R. H. Fish, *Angew. Chem., Int. Ed. Engl.*, 1997, **36**, 642; (d) J. R. Deschamps, C. M. Hartshorn, A. Singh and E. L. Chang, *Acta Crystallogr., Sect E*, 2002, **58**, m396; (e) N. J. Long, D. G. Parker, P. R. Speyer, A. J. P. White and D. J. Williams, *J. Chem. Soc., Dalton Trans.*, 2002, 2142.
- J. Hoorn, P. de Joode, W. L. Driessen and J. Reedijk, *Recl. Trav. Chim. Pays-Bas*, 1996, **115**, 191.
- (a) G. S. Matouzenko, A. Bousseksou, S. Lecocq, P. J. van Koningsbruggen, M. Perrin, O. Kahn and A. Collet, *Inorg. Chem.*, 1997, **36**, 2975; (b) O. Horner, E. Anxolabehere-Mallart, M.-F. Charlot, L. Tchertanov, J. Guilhem, T. A. Mattioli, A. Boussac and J.-J. Girerd, *Inorg. Chem.*, 1999, **38**, 1222.
- B. Dietrich, M. W. Hosseini, J.-M. Lehn and R. B. Sessions, *Helv. Chim. Acta*, 1985, **68**, 289.
- Using experimental conditions established by Buchwald and Hartwig: (a) J. P. Wolfe, S. Wagsaw and S. L. Buchwald, *J. Am. Chem. Soc.*, 1996, **118**, 7215; (b) F. Paul, J. Patt and J. F. Hartwig, *J. Am. Chem. Soc.*, 1994, **116**, 5969.
- O. Horner, M.-F. Charlot, A. Boussac, E. Anxolabehere-Mallart, L. Tchertanov, J. Guilhem and J.-J. Girerd, *Eur. J. Inorg. Chem.*, 1998, 721.
- C. J. Davies, S. J. Hilton, G. A. Solan, W. Stannard and J. Fawcett, *Polyhedron*, 2005, in press.
- See for example: (a) Y. Zang, J. Kim, Y. Dong, E. C. Wilkinson, E. H. Appelman and L. Que, Jr., *J. Am. Chem. Soc.*, 1997, **119**, 4197; (b) A. Diebold and K. S. Hagen, *Inorg. Chem.*, 1998, **37**, 215; (c) Z. He, D. C. Craig and S. B. Colbran, *J. Chem. Soc., Dalton Trans.*, 2002, 4224.
- I. Romero, M.-N. Collomb, A. Deronzier, A. Llobet, E. Perret, J. Pecaut, L. Le Pape and J.-M. Latour, *Eur. J. Inorg. Chem.*, 2001, 69.
- Mn...Mn distances for the ClMn(μ -Cl)₂MnCl motif, range: 3.786–3.887 Å, see for example: (a) ref. 17; (b) D. I. Arnold, F. A. Cotton, D. J. Maloney, J. H. Matonic and C. Murillo, *Polyhedron*, 1997, **16**, 133; (c) E. Sinn, *J. Chem. Soc., Dalton Trans.*, 1976, 162; (d) A. Garoufis, S. Kasselouri, S. Boyatziz and C. P. Raptopoulou, *Polyhedron*, 1999, **18**, 1615.
- D. Mandon, A. Machkour, S. Goetz and R. Welter, *Inorg. Chem.*, 2002, **41**, 5364.
- C. J. Davies, J. Fawcett and G. A. Solan, *Polyhedron*, 2004, **23**, 3105.
- W. L. F. Armarego and D. D. Perrin, *Purification of Laboratory Chemicals*, Butterworth, Heinemann, 4th edn., 1996.
- F. E. Mabbs and D. J. Machin, *Magnetism and Transition Metal Complexes*, Chapman and Hall, London, 1973.
- C. J. O'Connor, *Prog. Inorg. Chem.*, 1982, **29**, 203; *Handbook of Chemistry and Physics*, ed. R. C. Weast, CRC Press, Boca Raton, FL, 70th edn., 1990, p. E134.
- D. Astruc and J. R. Morow, *Bull. Chem. Soc. Fr.*, 1992, **129**, 319.
- T. Ukai, H. Kawazura, Y. Ishii, J. J. Bonnett and J. A. Ibers, *J. Organomet. Chem.*, 1974, **65**, 253.
- G. M. Sheldrick, *SHELXS97, program for crystal structure solution*, University of Göttingen, Germany, 1993.
- G. M. Sheldrick, *SHELXL97, program for crystal structure refinement*, University of Göttingen, Germany, 1993.